



TITLE:

f^{ϵ} SPECTRAL BEHAVIORS IN THE
AREA-PRESERVING TWO-DIMENSIONAL
MAPPINGS(Theory of Dynamical Systems
and Its Application to Nonlinear Problems)

AUTHOR(S):

Aizawa, Y.; Kohyama, T.

CITATION:

Aizawa, Y. ...[et al]. f^{ϵ} SPECTRAL BEHAVIORS IN THE AREA-PRESERVING TWO-DIMENSIONAL
MAPPINGS(Theory of Dynamical Systems and Its Application to Nonlinear Problems). 数理解析研究所講究録 1984, 536:
180-189

ISSUE DATE:

1984-09

URL:

<http://hdl.handle.net/2433/98675>

RIGHT:

$f^{-\nu}$ SPECTRAL BEHAVIORS
IN THE AREA-PRESERVING TWO-DIMENSIONAL MAPPINGS

Y. Aizawa and T. Kohyama

(相沢 洋 = 神山 保)

Department of Physics, University of Kyoto
Kyoto, Japan

ABSTRACT

This is the brief sketch about the non-markovian aspects observed in the chaotic motions of the area-preserving transformations. The asymptotic non-stationary behaviors are qualitatively characterized by the Allan variance, the power spectrum and the appropriate sojourn time distributions. The observed weak infrared catastrophe is explained by the symbolic renewal processes derived from the fractal structure of the phase space

1. Introduction

The $f^{-\nu}$ spectral behaviors of the ergodic dynamical systems are strongly correlated to some intermittent phenomena of the non-markovian class. Especially, concerning the one-dimensional intermittency, it became clear that many examples studied so far were successfully formulated in the framework of the semi-markovian renewal process.¹⁾ One of the interesting model is the modified Bernoulli system in the unit interval,

$$\begin{aligned}
\theta_{n+1} &= \theta_n + 2^{B-1}(1-2\varepsilon)\theta_n^B + \varepsilon & (0 \leq \theta_n < \frac{1}{2}) \\
\theta_n - 2^{B-1}(1-2\varepsilon)(1-\theta_n)^B - \varepsilon & & (\frac{1}{2} \leq \theta_n \leq 1)
\end{aligned} \tag{1}$$

where $\varepsilon (\geq 0)$ stands for a small perturbation and B is the positive bifurcation parameter. Taking the symbolic state σ ; $\sigma_n = -1$ for $0 \leq \theta_n < \frac{1}{2}$ and $\sigma = 1$ for $\frac{1}{2} \leq \theta_n \leq 1$, the time course of $\{\theta_n\}$ is simulated by the symbolic sequence $\{\sigma_n\}$. The jump events between $\sigma = -1$ and $\sigma = 1$ reveals strong intermittency for $B \geq 3/2$, as the result in the limit of $\varepsilon \rightarrow 0$, the power spectrum density $S(\omega)$ of $\{\sigma_n\}$ satisfies $S(\omega) \sim \omega^{-\nu}$ ($\omega \ll 1$) and the pausing time distribution of the state ($\sigma = -1$ or $\sigma = 1$) $P(m) \sim m^{-\beta}$ where $\beta = B/(B-1)$ and $\nu = 3 - \beta$. Above the infrared crisis limit at $B = 2$, the asymptotic non-stationary spectrum is observed as $\nu \geq 1$. This infrared catastrophe induces the non-stationary Allan variance $\sigma_A^2(\tau) \sim \tau^{2-\beta}$. This kind of infrared anomaly is originated from the fact that the orbit is strongly localized near the end points of the map ($\theta = 0$ or $\theta = 1$). In other words, the neighborhood of the points $\theta = 0$ and $\theta = 1$ are very sticky and the orbit is trapped there for extremely long time.

In the flow systems also, the same mechanism may induce the infrared anomaly. For instance, let us consider the oscillation in a double well potential with small dissipation, whose space profile is shown in Fig. 1.

Introducing the external periodic forcing, the homoclinicity induces the quite different ergodic motions depending on the tangential manner of the stable and unstable manifolds (Γ^+ & Γ^-). The symbolic

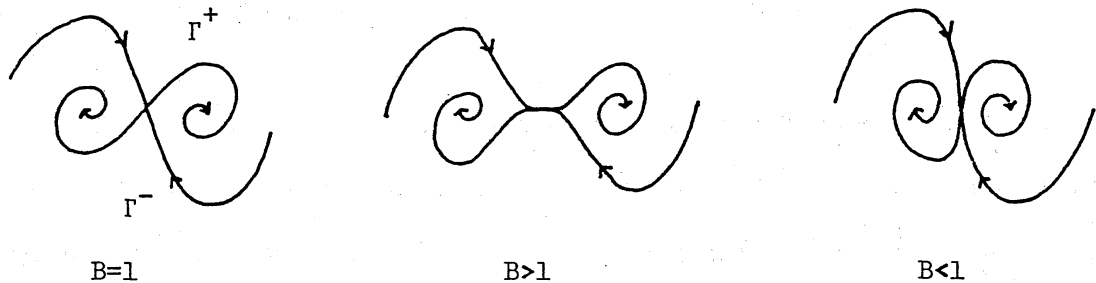


Fig.1 Various types of homoclinicity

sequence $\{\sigma_n\}$ is obtained from the following realization on the poincare section; $\sigma = -1$ for the left focussing motion and $\sigma = 1$ for the right. Each case in Fig.1 corresponds to the transversal ($B=1$), tangential ($B>1$), and inverse tangential ($B<1$) homoclinicity. The strong intermittency as was mentioned in the modified Bernoulli map is concerning to the tangential case.

Generally, the intermittency in the dissipative dynamical systems seems to appear via the weak homoclinicity.²⁾ However, in the area-preserving systems the other mechanism can induce the strong infrared anomalies. For an instance, let us consider the generic Hamiltonian systems, where the phase space is decomposed into many ergodic components; many kinds of KAM tori and stochastic regions. The essential point is that each KAM torus is the invariant set and that the neighborhood of them are very sticky. As the result the orbit stays near one of them for extremely long time before it departs to the other sticky zones. The existence of such wandering motions was pointed out

by Arnold.³⁾ Our problem is to estimate the statistical properties of such motions. In what follows, we will discuss some numerical results showing the infrared anomalies. From the mathematical viewpoint, the measure theoretic aspect of such sticky zones are difficult to identify even in the perturbation approach,⁴⁾ but in the practical viewpoint the computer simulations enable us to predict the long time behaviors of them so long as the sticky zones are metrically transitive after the last KAM tori disappear.

The recent studies on the one-dimensional systems show that the statistical quantities such as correlation functions and power spectrum depend sensitively on the topological structures of the systems.⁵⁾ In the high dimensional cases also, the detail topological informations are necessary in order to reach the theoretical goal. In the dynamical system with two degrees of freedom, however, the topological characters are relatively simple on the area-preserving poincare section as the twist map, where the rotation mechanism is dominant.⁶⁾ The purpose of the present articles is to explain the symbolic dynamics approach to the infrared anomalies of the two dimensional case. The higher dimensional cases are still open, where the detail mechanisms such as the Arnold diffusion must be taken into account when we construct the symbolic dynamics.

2. Fractal Geometry of Phase Space

As was clearly stated by Zehnder, the generic aspects of the phase space is quite fractal.⁷⁾ The infinite many KAM regions are hierarchically distributed in the phase space. An arbitrary KAM region is

surrounded by a certain stochastic zone, and the center of each KAM region is an elliptic point. Near the hyperbolic point, the chaotic orbit appears via homoclinicity.

Among the various KAM hierarchies, we take note of a main series of KAM regions (Fig.2), and denote the class of the KAM tori by an integer k ($=0,1,2,\dots$). As is shown in Fig.2, the tori of the class k is distributed around a $(k-1)$ th KAM torus, and simultaneously surrounded by the $(k+1)$ th tori. The hierarchical structure illustrated in Fig.2 continues self-generatively to infinite small scale. Each KAM region in the main series is further divided into many sub-series of the finer KAM tori. In what follows, however, our discussion will be limited only to the main series mentioned above.

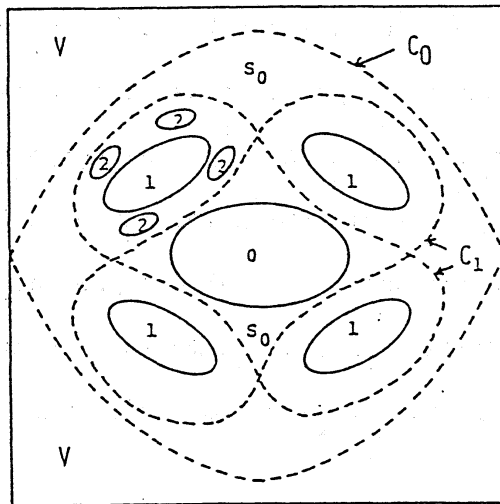


Fig.2

Schematic picture of the hierarchical structure of phase space. Circles are the outer boundaries of the KAM tori of the main series. Dotted lines are the ghost separatrices.

A KAM region of class k is assumed to be packed in the imaginary separatrix that is the vestige of the integrable case approximating our mode. The stochastic region surrounded by the separatrix is denoted by S_k and C_k where $C_k = S_k + C_{k+1}$. The whole stochastic regimes of our model

is $\bigcup_{k=0}^{\infty} S_k + V$, where V is the space outside C_0 .

The motion in the stochastic regime is described by a symbolic sequence of the ranking number m of S_m to which the orbital point is included. Denoting the mapping time by n , the symbolic dynamics is constructed,

$$\begin{aligned} \psi : m(n) &\rightarrow m(n+1) \\ (n = \text{integer and } m &= -1, 0, 1, \dots) \end{aligned} \quad (2)$$

The state $m = -1$ means that the point is in V .

The following assumptions are used; (I) the number of the cluster C_k is ρ^k , (II) the phase volume of C_k satisfies $\text{vol}[C_k] = b \cdot \text{vol}[C_{k+1}]$, and (III) ρ^k clusters of C_k have a certain self-similar structure for all k . From these assumptions, the joint probability $P(m, n)$ for the state m with the pausing time n is derived,⁶⁾

$$\begin{aligned} P(m, n) &\simeq P(m) \cdot n^{-D} \\ (D = \frac{\ln b}{\ln \rho} \text{ and } P(m) &\sim (\rho/b)^m) \end{aligned} \quad (3)$$

3. Semi-markovian Process and the Infrared Anomaly

The jump probability $P_{m,k}$ from the state m to the k is determined by,

$$\sum_m P(m) P_{m,k} = P(k) \quad (4)$$

The most simple case is that the jump event occurs among two successive clusters m and $m \pm 1$, then

$$P_{m,k} = \frac{1}{2} \pm \frac{b-\rho}{2(b+\rho)} \quad , \quad (k=m+1) \quad . \quad (5)$$

Equations (3) and (5) uniquely determines a semi-markovian process which simulates the symbolic dynamics of eq.(2).

As the direct result of the Pareto-Zipf law about the pausing time distribution, the infrared anomalies mentioned in §1 are induced. For an example, let us consider the fluctuation of the rotation number $\theta(n)$ around the primary KAM torus. The Allan variance $\sigma_A^2(\tau)$ and the power spectrum $S(\omega)$ for $\theta(n)$ are estimated,

$$\begin{aligned} \sigma_A^2(\tau) &\sim \tau^{2-D} \\ S(\omega) &\sim \omega^{D-3} \end{aligned} \quad (6)$$

4. Numerical Results

The standard mapping, which describes the poincare section for the parametrically driven pendulum, is studied.

$$I_{n+1} = I_n - \frac{K}{2\pi} \sin(2\pi\theta_n) \quad (7)$$

$$\theta_{n+1} = \theta_n + I_{n+1}$$

Figure 3 shows the orbital points obtained by the iteration of the map. The white parts are the KAM regions. The power spectrum $S(\omega)$ and the Allan variance $\sigma_A^2(\tau)$ are calculated for the dynamical variable $\cos(2\pi\theta_n)$ near the bifurcation parameter $K=1.5$ (Fig.4). The infrared anomalies such as $S(\omega) \sim \omega^{-\nu}$ and $\sigma_A^2(\tau) \sim \tau^\gamma$ are clearly observed, where $\nu=\gamma+1$.

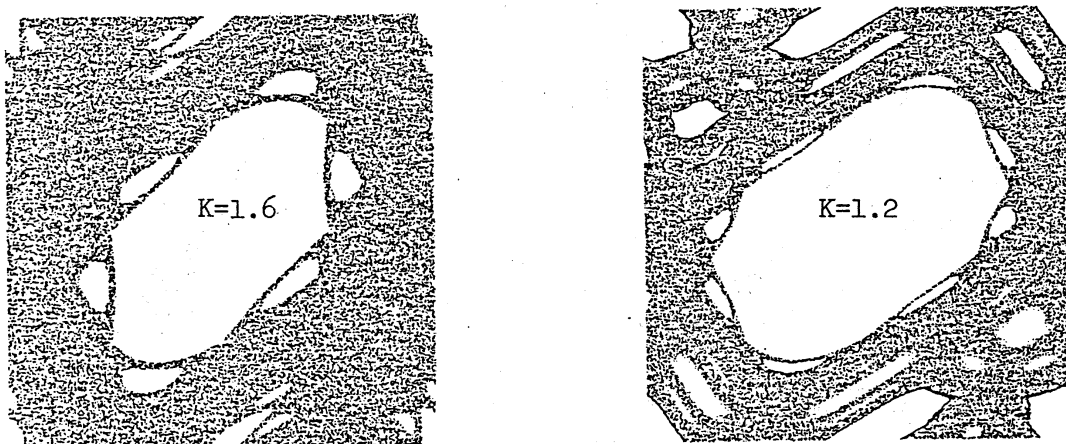
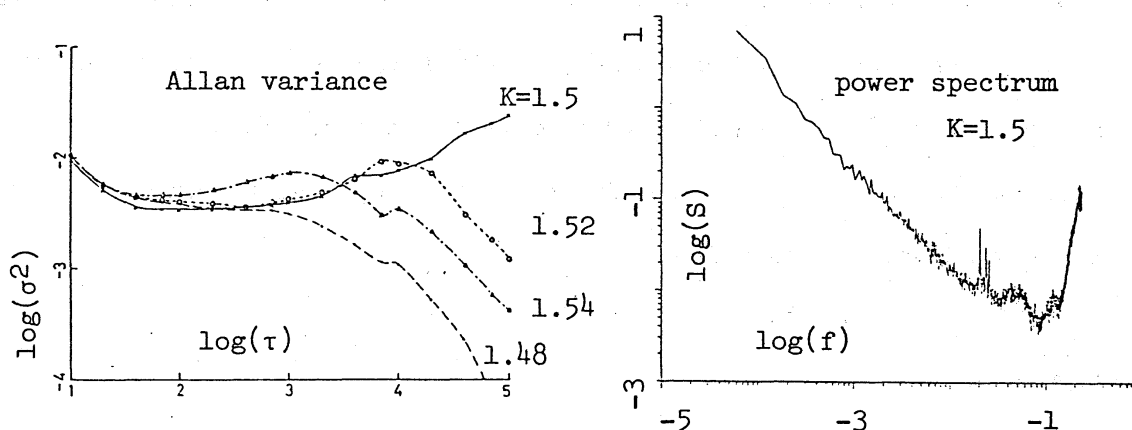
Fig.3 Poincare section in (θ, I) space

Fig.4 Allan variance and power spectrum density

The pausing time distribution $P(n)$ is calculated from the sojourn time around the primary cluster. Figure 5 shows the Pareto-Zipf law $P(n) \sim n^{-D}$. These numerical results reveals the well accordance with the theoretical ones predicted in §3.⁸⁾

The mechanism for the infrared anomalies in the area-preserving map is quite different from that in the one-dimensional map such as in the modified Bernoulli system, but the interrelation among various

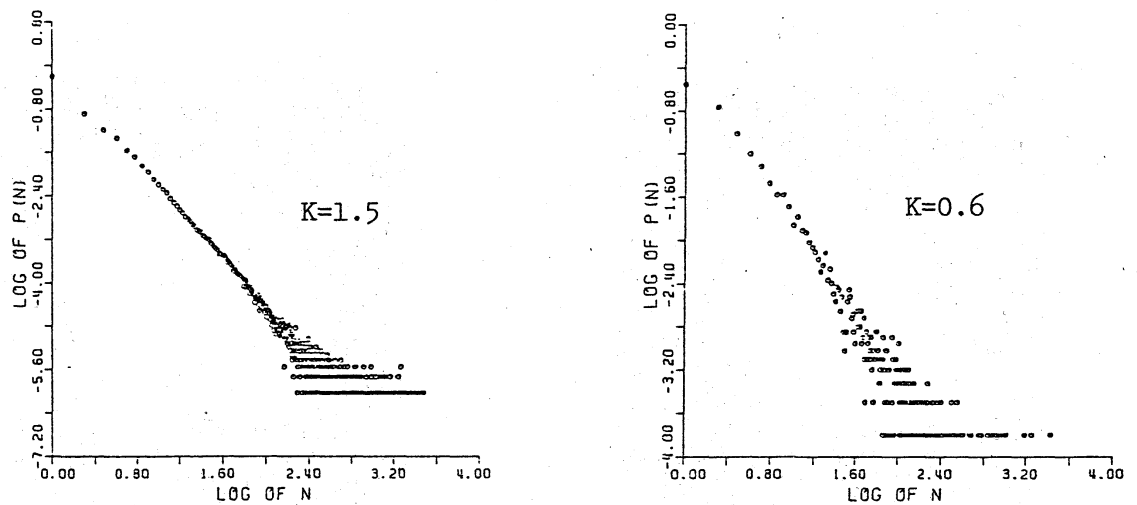


Fig.5 pausing time distribution

indices is the same in both cases. This suggests that the study on the intermittency should be extended to that of the heterogeneous random geometry beyond the ordinary time series analysis. This direction seems to be parallel to the problems in the critical phenomena and in the hydrodynamical turbulence.

References

- 1) Y. Aizawa, C. Murakami and T. Kohyama, 'Statistical Mechanics of Intermittent Chaos', Prog. Theor. Phys. Supple. 79 (1984), to appear.
- 2) T. Uezu & Y. Aizawa, 'Some Routes to Chaos from Limit Cycle in the Forced Lorenz System', Prog. Theor. Phys. 68 No.5 (1982), 1543.
- 3) V.I. Arnold & A. Avez, 'Problèmes Ergodiques de la Mécanique Classique', (Gauthier-Villars, 1968).
- 4) V.I. Arnold, 'Instability of Dynamical Systems with Several Degrees of Freedom', Sov. Math. Dokl. 5 No.3 (1964), 581.

- 5) H. Mori, B.C. So and T. Ose, 'Time correlation Function of One-dimensional Transformations', Prog. Theor. Phys. 66 No.4 (1981), 1266.
- 6) Y. Aizawa, 'Symbolic Dynamics Approach to the Two-Dimensional Chaos in Area-Preserving Maps', Prog. Theor. Phys. 71 No.6 (1984), in press.
- 7) E. Zehnder, 'Homoclinic Points Near Elliptic Fixed Points', Commun. Pure and Appl. Math. XXVI, (1973), 131.
- 8) T. Kohyama, 'Non-Stationality of Chaotic Motions in an Area-Preserving Mapping', Prog. Theor. Phys. 71 No.5 (1984), 1104.